

Critical phenomena and giant superparamagnetic moments above Curie point of the amorphous $\text{Fe}_{20}\text{Ni}_{60}\text{P}_{14}\text{B}_6$ alloy

S. N. Kaul

Institut für Experimentalphysik IV, Ruhr Universität Bochum, 4630 Bochum, West Germany

(Received 1 May 1980)

Results of the magnetization measurements performed on the amorphous $\text{Fe}_{20}\text{Ni}_{60}\text{P}_{14}\text{B}_6$ alloy in the temperature range 210 to 255 K in fields up to 10 kOe are reported. Magnetic data taken in the critical region, when analyzed with caution, give the values for the Curie temperature and critical exponents β , γ , and δ as 227.7 ± 0.5 K, 0.39 ± 0.02 , 1.33 ± 0.05 , and 4.45 ± 0.07 , respectively. A close agreement between the above exponent values and those derived from the theories based on a three-dimensional Heisenberg model suggestive of the dominant short-range forces in the critical region (long-range forces, e.g., dipolar forces are shown to have negligible effect on the critical fluctuations of magnetization) has been observed. The data satisfy the magnetic equation of state characteristic of a second-order phase transition over the entire temperature range of the present investigation. A detailed analysis of the magnetization versus field isotherms taken above T_C reveals the existence of giant superparamagnetic clusters in the present alloy for temperatures above T_C . A small peak, which shifts to higher temperatures when the field strength is increased, observed in the magnetization versus temperature curves above T_C for fields ≤ 100 Oe has been shown to arise from the freezing of the ferromagnetic order within the giant clusters. Finally, a physical basis is provided for observing different values for the ferromagnetic ordering temperature as determined by a local measurement like the Mössbauer effect, on one hand, and resistivity and the present bulk magnetic measurements, on the other.

I. INTRODUCTION

Complete failure^{1,2} of the mean-field theory to arrive at correct numerical values for the critical indices in two and three dimensions has triggered immense theoretical as well as experimental activity in the field of critical phenomena. During the last two decades, a large number of theoretical investigations on critical phenomena employing renormalization-group, high-temperature series expansion, cumulant expansion, and Monte Carlo techniques in the Ising and Heisenberg spin models have appeared in the literature,²⁻¹⁶ and the detailed magnetic studies in the critical region performed on ferromagnets in the crystalline state¹⁷⁻²⁵ have shown that the experimental values of the critical exponents follow closely predictions of the theories based on a three-dimensional Heisenberg model. Recently considerable interest has been shown in a similar comparison between theory and experiment in amorphous ferromagnetic systems.²⁶⁻³³ A study of this type (motivated primarily by the basic questions such as: Do the amorphous ferromagnetic systems, like their crystalline counterparts, exhibit a second-order magnetic phase transition and if so, how does a total loss of crystalline symmetry in these materials affect the critical behavior?) already carried out on amorphous $\text{Co}_{70}\text{B}_{20}\text{P}_{10}$, $\text{Fe}_{80}\text{P}_{13}\text{C}_7$, $\text{Fe}_{32}\text{Ni}_{36}\text{Cr}_{14}\text{P}_{12}\text{B}_6$ (Metglas 2826A), $\text{Fe}_{29}\text{Ni}_{49}\text{P}_{14}\text{B}_6\text{Si}_2$

(Metglas 2826B), and $\text{Gd}_{80}\text{Au}_{20}$ alloys²⁶⁻³³ shows that these systems exhibit a well-defined magnetic phase transition with the reduced magnetization and field following an equation of state derived for second-order phase transition^{4-6, 15, 34-37} and with the critical exponents satisfying an equality relation resulting from the static scaling law.^{4, 35-37} Like crystalline systems, these alloys (except for Metglas 2826B) also give critical exponent values in striking agreement with those derived for a three-dimensional Heisenberg model. However, for all the amorphous materials studied so far it is observed that the value of the exponent β tends to be close to 0.4 (Refs. 30 and 33) rather than to the value 0.37 generally accepted for the Heisenberg model. It is, therefore, imperative to establish whether such a trend is representative of only the few above-mentioned systems or is it maintained for all other amorphous ferromagnetic alloys as well?

Understanding of the physical mechanisms involved in spin-glass, mictomagnetic and superparamagnetic regimes as progressive steps of magnetic ordering between the Kondo concentration and the critical concentration for the onset of a long-range homogeneous ferromagnetic ordering in transition-metal-metalloid amorphous alloys has become particularly important because the complex nature of these intermediate magnetic regimes is found to have a

direct bearing^{33,38-41} on the so-called "resistivity-minimum paradox" associated with such systems. Such an investigation carried out only on the amorphous systems like $(\text{Fe,Pd})_{80}\text{P}_{20}$, $(\text{Fe,Pd})_{80}\text{Si}_{20}$, $(\text{Fe,Ni})_{79}\text{P}_{13}\text{B}_8$, and $(\text{La,Gd})_{80}\text{Au}_{20}$ alloys³⁹⁻⁴¹ is still in its infancy. Recently, the amorphous $\text{Fe}_x\text{Ni}_{80-x}\text{P}_{14}\text{B}_6$ alloy series has attracted the attention of a number of workers for a similar type of study. Mössbauer data⁴² taken on this system reveal a critical concentration above which ferromagnetism appears as $x_c \approx 8$, a spin-glass-type behavior for the alloy with $x = 10$ and above this concentration a normal long-range ferromagnetic ordering. From low-temperature specific-heat and magnetic-susceptibility measurements,⁴³ a typical spin-glass behavior has been observed for alloys with $x = 3, 5$ whereas the alloy with $x = 7$ has been found to exhibit a mictomagnetic behavior. A comprehensive magnetic study³⁸ of the amorphous $\text{Fe}_{10}\text{Ni}_{70}\text{P}_{14}\text{B}_6$ alloy demonstrates that in this alloy, both spin-glass and mictomagnetic properties, existing for temperatures below ~ 45 K, are accompanied above this temperature by a characteristic superparamagnetic behavior. Magnetoresistance results⁴⁴ indicate that the tendency towards the formation of superparamagnetic clusters in this alloy system extends up to the highest concentration studied, i.e., $x = 13$, while the specific-heat and resistivity⁴⁵ studies support an inhomogeneous long-range ferromagnetic behavior in the $\text{Fe}_{20}\text{Ni}_{60}\text{P}_{14}\text{B}_6$ alloy. Though a long-range ferromagnetic ordering has been reported for $x \geq 30$,⁴⁶ there exist in the literature no magnetic data for the intermediate concentration range $10 < x < 30$ to throw light on the critical concentration for the onset of a homogeneous long-range ferromagnetism in the amorphous $\text{Fe}_x\text{Ni}_{80-x}\text{P}_{14}\text{B}_6$ alloy system.

We chose to study in detail the magnetic behavior of the amorphous $\text{Fe}_{20}\text{Ni}_{60}\text{P}_{14}\text{B}_6$ alloy in the critical region for the following reasons: (i) to establish whether the general trend which the exponent β exhibits in the amorphous materials studied previously is also maintained in the present alloy; (ii) to arrive at the critical concentration for the onset of a homogeneous long-range ferromagnetic ordering in the amorphous $\text{Fe}_x\text{Ni}_{80-x}\text{P}_{14}\text{B}_6$ system; (iii) to ascertain whether this alloy exhibits an inhomogeneous long-range ferromagnetic behavior as suggested by the indirect measurements, namely, resistivity and specific heat; and finally (iv) the fact that the Curie temperature of this alloy lies well below its crystallization temperature allows us to perform such a study without any complications due to the structural relaxation effects.

In this paper, the results of magnetization measurements performed on amorphous $\text{Fe}_{20}\text{Ni}_{60}\text{P}_{14}\text{B}_6$ alloy in the temperature range 210 to 255 K in fields up to 10 kOe are reported. Determination of the spontaneous magnetization and initial susceptibility

values at different temperatures in the critical region from the Arrott plots permits evaluation of the critical exponents and the Curie temperature. A close agreement, suggestive of the dominance of the short-range forces in the critical region, is found between the experimental critical exponent values and the corresponding theoretical values deduced for a three-dimensional Heisenberg model. Marked non-linearity in the Arrott plots, resulting in large deviation of the data points from the asymptotic behavior dictated by the magnetic equation of state for fields ≤ 700 Oe, has been attributed to superparamagnetism in this alloy and a detailed analysis of the magnetization-versus-field isotherms taken at different temperatures above the Curie temperature T_C demonstrates clearly the existence of giant superparamagnetic clusters. In addition, a clear physical insight into the different ferromagnetic ordering temperatures obtained for this alloy from previous Mössbauer and resistivity measurements on one hand, and from the present bulk magnetization measurements on the other, is provided. It is observed that the present alloy exhibits an inhomogeneous long-range ferromagnetic ordering and represents a composition in the amorphous $\text{Fe}_x\text{Ni}_{80-x}\text{P}_{14}\text{B}_6$ alloy series just above the percolation concentration.

II. EXPERIMENTAL RESULTS AND DISCUSSION

The magnetization measurements were made on the amorphous $\text{Fe}_{20}\text{Ni}_{60}\text{P}_{14}\text{B}_6$ alloy ribbons of about 1.25 mm width and 0.03 mm thickness employing Faraday method and a procedure described in detail elsewhere.^{33,38} With the external magnetic field directed along the ribbon breadth and the temperature increasing from 210 K at a rate of 0.5 K/min, the magnetization as a function of temperature was measured for constant external fields up to 10 kOe in the temperature interval between 210 and 255 K. The relative accuracy of the present measurements was found to be better than 0.1%.

The results of the temperature dependence of magnetization taken at various constant values of the external magnetic field in the temperature range 210 to 255 K are depicted in Figs. 1 and 2. These figures show clearly that the present alloy exhibits a well-defined magnetic phase transition at $T_C = 228$ K, obtained from the kink observed in the magnetization-versus-temperature curve taken at 28.5 Oe (see Fig. 1). With increasing field strength the kink point shifts to lower temperatures, as is usually observed in ferromagnetics in crystalline or amorphous state. Furthermore, for low values of the external field ≤ 100 Oe, magnetization as a function of temperature above T_C is seen in Fig. 1 to go through a peak (observed only when full resolution of the apparatus

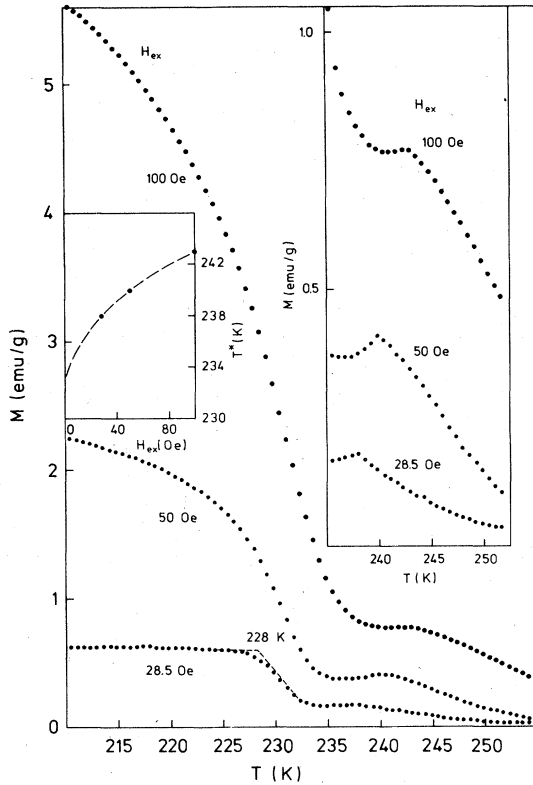


FIG. 1. Magnetization as a function of temperature for constant external magnetic field values of 28.5, 50, and 100 Oe. The left-hand-side insert in this figure depicts the variation of the peak position T^* with the external field H_{ex} whereas the right-hand-side insert shows magnetization plotted against temperature on a very sensitive scale in the temperature range 235 to 252 K.

is used) which shifts to higher temperatures as the field value is progressively increased from 28.5 Oe. The above observation is made obvious by plotting magnetization on a very sensitive scale in the temperature region 235–252 K in the right-hand-side insert of Fig. 1. For reasons which will be clear later on, we defer the physical interpretation of such a peak in magnetization-versus-temperature curves until the later part of this section and instead proceed to evaluate the critical exponent values with a view to establish whether or not the phase transition in the present alloy manifests a second-order magnetic phase transition as evidenced previously in crystalline systems and in some amorphous alloys. However, before embarking upon such a venture, it seems necessary to define in brief the critical exponents, the static scaling law and the magnetic equation of state.

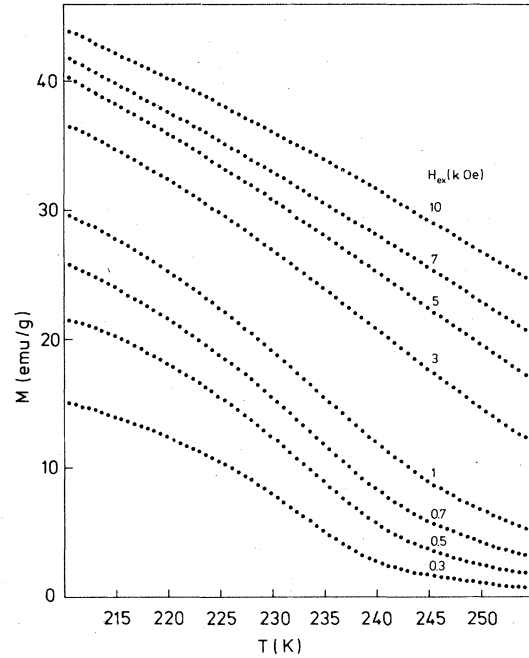


FIG. 2. The temperature dependence of magnetization for constant external magnetic fields ($0.3 \leq H_{ex} \leq 10$ kOe) in the temperature region 210 to 255 K.

A. Critical exponents, static scaling relation between them and magnetic equation of state

The second-order phase transition around the Curie point T_C is known^{3,6,10,15} to be characterized by a set of critical exponents (β , γ , and δ) and a magnetic equation of state. The temperature dependence of the spontaneous magnetization $M_s = \lim_{H \rightarrow 0} M$ just below T_C is governed by β through the relation

$$M_s = A_- [1 - (T/T_C)]^\beta \quad (1)$$

and that of the inverse initial susceptibility $\chi_0^{-1} = \lim_{H \rightarrow 0} (H/M)$ just above T_C by γ through the relation

$$\chi_0^{-1} = A_+ [(T/T_C) - 1]^\gamma \quad (2)$$

The exponent δ relates M and H at T_C as

$$M = BH^{1/\delta} \quad (3)$$

The static scaling hypothesis developed by several authors^{4,35-37} gives the following relation between the exponents β , γ , and δ :

$$\delta = 1 + (\gamma/\beta) \quad (4)$$

and thereby demonstrates the fact that only two of the three exponents are independent. The magnetic equation of state^{4-6, 15, 34-37} in the critical region in its simplest form can be written as

$$h/m = f_{\pm}(m) , \quad (5)$$

where the plus and minus signs denote temperatures above and below T_C , respectively, $m \equiv M/|\epsilon|^{\beta}$ is the reduced magnetization and $h \equiv H/|\epsilon|^{\beta+\gamma}$ the reduced field with $\epsilon = (1 - T/T_C)$. Equation (5) implies that h/m as a function of m falls on two different universal curves: $f_{-}(m)$ for temperatures below T_C and $f_{+}(m)$ for temperatures above T_C .

1. Critical exponents

Equations (1) and (2) clearly show that the computation of the values for the critical exponents β and γ needs evaluation of M_s and χ_0^{-1} as functions of temperature, respectively. Following the conventional method, based on the molecular-field theory and developed by Arrott⁴⁷ and Kouvel,⁴⁸ the values of M_s and χ_0^{-1} at different temperatures have been determined, respectively, from the intercepts along M^2 axis (i.e., $H/M = 0$) and H/M axis (i.e., $M^2 = 0$) of the M^2 versus H/M plots made at different temperatures below and above T_C . However, some caution is needed to use such plots because the normal procedure of obtaining M_s simply by extrapolating the linear high-field portion to $H/M = 0$ leads to erroneous results⁴⁹ so far as the true values of M_s and T_C are concerned. A better procedure,^{49, 50} which gives the value of T_C determined from the Arrott-Kouvel plot in agreement with the values obtained by other techniques, namely, kink-point method and magneto-caloric effect, is to employ a parabolic extrapolation of the M^2 vs H/M curves instead of a linear one. Consequently, we adopt this procedure to evaluate the temperature dependence of M_s and χ_0^{-1} from the plots given in Fig. 3. This figure shows M^2 vs H/M curves (where H has already been corrected for the demagnetizing field) plotted at 1.25-K intervals (for clarity sake) in the temperature range 210.5 to 250.5 K and gives the value for T_C as 228 K, which is in excellent agreement with that obtained by the kink-point method. In order to minimize errors inherent in such extrapolation techniques, M^2 as a function of H/M was plotted on a very sensitive scale at temperature intervals of about 0.6 K in the above temperature range and the temperature dependence of M_s and χ_0^{-1} obtained thereby is shown in Figs. 4 and 5, respectively. Equations (1) and (2) can be written in an alternative form as

$$\left(\frac{d(\ln M_s)}{dT} \right)^{-1} = M_s \left(\frac{dM_s}{dT} \right)^{-1} = (T - T_C)/\beta \quad (6)$$

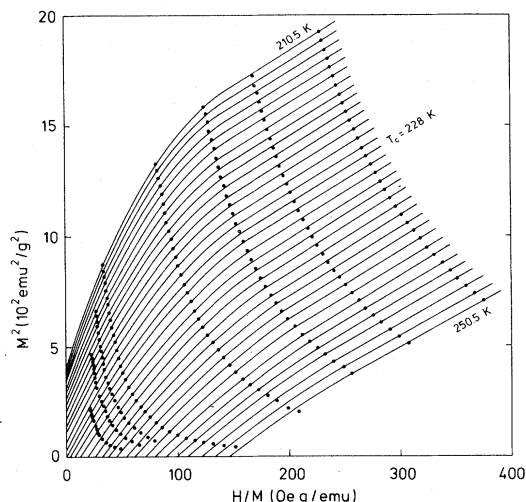


FIG. 3. M^2 vs H/M plots made at 1.25-K intervals in the temperature range 210.5 to 250.5 K give value for T_C as 228 K. Intercepts with M^2 and H/M axes give the values of spontaneous magnetization and inverse initial susceptibility at different temperatures, respectively.

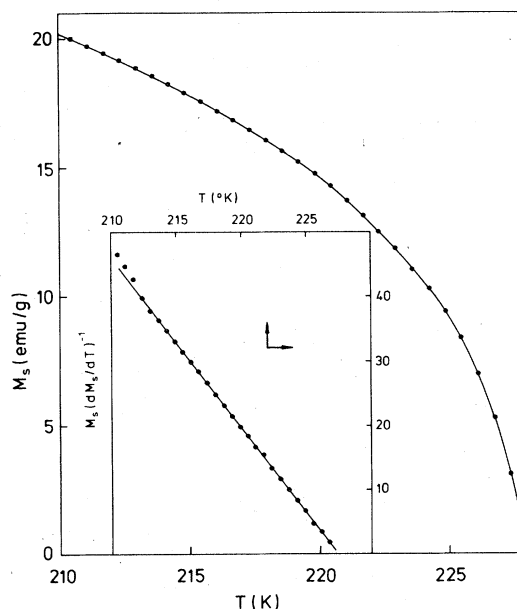


FIG. 4. Spontaneous magnetization M_s as a function of temperature. Insert shows plot of $M_s(dM_s/dT)^{-1}$ vs temperature which gives the critical exponent β and Curie temperature (see text).

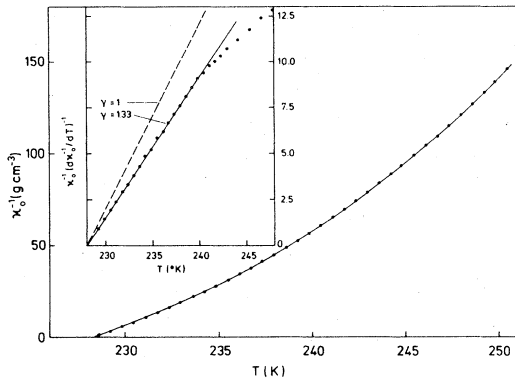


FIG. 5. Temperature dependence of the inverse initial susceptibility χ_0^{-1} . Insert shows the $\chi_0^{-1}(d\chi_0^{-1}/dT)^{-1}$ vs temperature plot which gives the critical exponent γ and Curie temperature (see text).

and

$$\left(\frac{d(\ln\chi_0^{-1})}{dT}\right)^{-1} = \chi_0^{-1} \left(\frac{d\chi_0^{-1}}{dT}\right)^{-1} = (T - T_C)/\gamma \quad (7)$$

It is evident from these equations that the plots of $M_s(dM_s/dT)^{-1}$ vs T and $\chi_0^{-1}(d\chi_0^{-1}/dT)^{-1}$ vs T should be straight lines with slopes $(1/\beta)$ and $(1/\gamma)$, respectively, and such straight lines when extrapolated to ordinate equal to zero should yield intercepts on their T axes equal to the Curie temperature. According to Kouvel and Fisher,¹⁷ the above-mentioned plots, shown in the inserts of Figs. 4 and 5, give precise values of T_C , β , and γ . However, certain sources of error deserve proper attention. First, small variations are possible while drawing a smooth curve through M_s or χ_0^{-1} data points. Second, the temperature T at which the local derivative dM_s/dT or $d\chi_0^{-1}/dT$ is defined as uncertain to within ± 0.05 K. Also, due consideration should be given to the accuracy limit ± 0.05 K of the temperature measurement. All these combined together give two-dimensional uncertainty limits which are included in the size of the close-circled points in the inserts of Figs. 4 and 5. The straight lines obtained from a least-squares fit through the centers of the data points in these inserts give values of $\beta = 0.39$, $T_C = 227.4$ K and $\gamma = 1.33$, $T_C = 228$ K, respectively. In order to evaluate the limits of uncertainty in these values, the least-squares fits through the edges of the data points are made to yield $\beta = 0.39 \pm 0.02$, $T_C = 227.4 \pm 0.2$ K and $\gamma = 1.33 \pm 0.05$, $T_C = 228.0 \pm 0.2$ K. Large deviations of the data points from the linear fit corresponding to $\gamma = 1.33$ apparent in the insert of Fig. 5 above 241 K point to the fact that the values of γ increases continuously even up to 255 K (this plot has been extended to 255 K to test the validity of this statement) contrary to the usual observation¹⁷ that

above T_C γ decreases smoothly with temperature and approaches unity at a temperature beyond which Curie-Weiss law is obeyed. A dashed line corresponding to $\gamma = 1$ is included in this insert to elucidate the above finding which, in turn, suggests that a short-range magnetic order persists for temperatures well above T_C .

In Fig. 6, $\ln M$ is plotted against $\ln H$ for the T_C values obtained from Figs. 4 and 5, i.e., 227.4 and 228 K. It is evident from Fig. 6 that Eq. (3) is valid for fields in excess of 700 Oe (lower the field value than 700 Oe, more the magnetization values deviate from these least-squares straight-line fits) with $\delta = 4.49$ and 4.40 for 227.4 and 228 K, respectively. Although such deviations at low values of the field can, in part, be attributed to the difficulty in estimating the correct value for the demagnetizing field and to the "rounding effect" due to the finite size¹⁶ of the samples, a more plausible explanation is given in the later text. Validity of Eq. (3) in a wide temperature range suggests the following relation between T_C and δ .

$$T_C = 228.0 - 6.667(\delta - 4.40) \quad (8)$$

A relation similar to Eq. (8) has been previously observed by Arrott and Noakes²⁰ for crystalline Ni but with the coefficient of the second term about 40 times smaller in magnitude than that given in Eq. (8). The above comparison indicates that in their case δ is about 40 times more sensitive to the choice of T_C than that found for the present alloy. It is, therefore, not surprising to note that relatively large uncertainty limits are associated with our values for T_C and δ . Using the value of $T_C = 227.7 \pm 0.5$ K (ob-

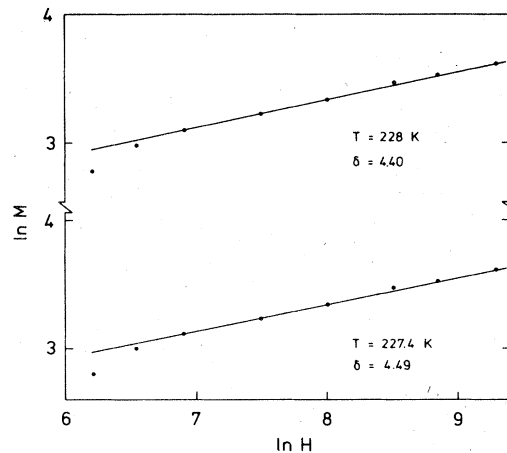


FIG. 6. $\ln M$ vs $\ln H$ plots for 227.4 and 228 K. The slope of the least-squares-fit straight lines through the data points gives the values for the exponent δ as 4.49 and 4.40 for temperatures 227.4 and 228 K, respectively.

tained from the maximum error limits deduced previously from Figs. 4 and 5) in Eq. (8), the value of δ without any loss of accuracy comes out to be 4.45 ± 0.07 . Substitution of the values $\beta = 0.39 \pm 0.02$ and $\gamma = 1.33 \pm 0.05$ in Eq. (4) yields $\delta = 4.41 \pm 0.3$, which is in conformity with its presently determined value. The value of the specific-heat exponent α computed from the relation $\alpha = 2(1 - \beta) - \gamma$ is found to be -0.11 ± 0.01 .

The present values for the critical exponents conform reasonably well with the values $\beta \approx 0.37$, $\gamma \approx 1.37$, $\delta \approx 5.0$, and $\alpha \approx -0.1$ predicted by theories based on a three-dimensional Heisenberg model. Close agreement between the experimental and theoretical values implies that the short-range forces dominate in the critical region. In order to rule out any influence from the long-range forces (e.g., dipolar forces), we use the criterion of Kadanoff *et al.*² that the effect of long-range forces on the critical fluctuations of magnetization can be neglected in case

$$\epsilon \gg [\mu M_s(0)/kT_C]^{1/\beta(\delta-1)} \equiv t, \quad (9)$$

where $\mu = g\mu_B S$ is the moment per spin and $M_s(0)$ the saturation magnetization at 0 K. The value of " t " for Fe and Ni calculated using their S and $M_s(0)$ values is found to be 0.002 and 0.003, respectively. Experimentally, we have determined the critical exponents for the present alloy in the regions $|\epsilon| = 0.066$ for $T < T_C$ and 0.057 for $T > T_C$. Considering the fact that $|\epsilon| \sim 25t$, the agreement between the present and Heisenberg values is not at all surprising. Furthermore, long-range forces are expected to be significantly reduced in amorphous materials with a very short mean-free path.⁵¹

2. Magnetic equation of state

In the limit of large m (i.e., when the thermal effect is dominated by the field effect) the magnetic equation of state given by Eq. (5) reduces to $f_{\pm}(m) \propto m^{\delta-1}$ and in a sense represents another version of Eq. (3) which is normally valid for small m . For small m the thermal and magnetic field effects become equally important and hence materials with different magnetic properties give different asymptotic forms experimentally. However, the general asymptotic form which has gained sufficient recognition^{19,21,30} over the years is given by

$$h/m = \pm a_{\pm} + b_{\pm} m^2, \quad (9)$$

where plus and minus signs have the usual meaning. We, therefore, plot m^2 vs h/m in Fig. 7 and define the intercepts of the curves obtained thereby with the m^2 and h/m axes as m_0^2 and h_0/m_0 , respectively. Using the definition of the reduced field, h , and reduced magnetization, m , it is easy to show that the coeffi-

icients in Eq. (9) are related to the coefficients in Eqs. (1) and (2) as follows:

$$a_+ = A_+ = h_0/m_0, \quad T > T_C$$

and

$$(a_-/b_-)^{1/2} = A_- = m_0, \quad T < T_C. \quad (10)$$

Figure 7 clearly demonstrates the validity of Eq. (5) over a wide temperature range and gives the values for the intercepts h_0/m_0 and m_0 as $2.88 \pm 0.08 \times 10^3$ Oe g/emu and 52.92 ± 0.45 emu/g, respectively. The central dash-dot line represents the asymptotic form of the two universal curves for large m . Equation (10) has been used to cross check the intercept values obtained from Fig. 7 so as to gain more confidence in them. The values of the coefficients A_+ and A_- determined from the intercept values on the ordinates of the log-log plots of χ_0^{-1} vs $|1 - T/T_C|$ and M_s vs $|1 - T/T_C|$, respectively, are found to be 2.88×10^3 Oe g/emu and 52.84 emu/g, in close conformity with the previously evaluated values of h_0/m_0 and m_0 .

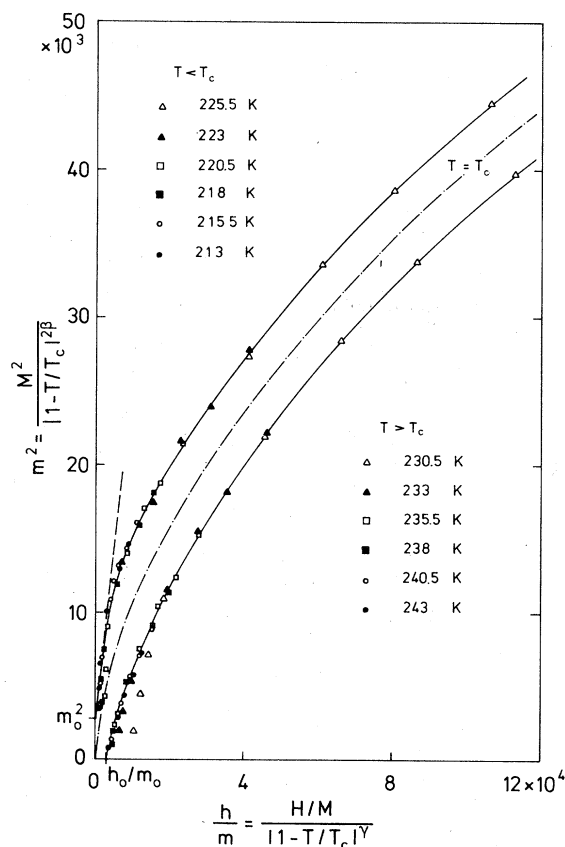


FIG. 7. Square of reduced magnetization $m^2 = M^2/|1 - T/T_C|^{2\beta}$ vs reduced inverse susceptibility $h/m = (H/M)/|1 - T/T_C|^\gamma$ for temperatures below and above Curie temperature T_C , where M is in emu/g and H in Oe. The dash-dot line indicates the asymptotic behavior of the two universal curves for large m .

At this stage it seems worthwhile to mention that marked deviations (not very apparent from Fig. 7) from the universal curves result for fields ≤ 700 Oe. Such deviations, however, become quite evident when the log-log plots of $(m^2 - m_0^2)$ vs h/m and m^2 vs $[(h/m) - (h_0/m_0)]$ shown in Fig. 8 are made to check the formerly established asymptotic relations [Eq. (9)] for small m . In this figure universal curves for temperatures above and below T_C are seen to approach the asymptotic behavior for large m given by the dashed lines. Deviations of the above nature observed throughout the present investigation originate basically from the strong nonlinearity in the Arrott plots (Fig. 3) and hence signal the presence of superparamagnetic clusters due to either chemical inhomogeneities or magnetic polarization clouds.^{52,53} Additional evidence supporting this point of view is provided by the following observations: (i) persistence of the short-range magnetic order for temperatures well above T_C as evidenced by the deviation of the data points from the straight-line relationship between $\chi_0^{-1}(d\chi_0^{-1}/dT)^{-1}$ and T for temperatures in excess of 241 K (insert in Fig. 5); (ii) M_s vs T and χ_0^{-1} vs T curves do not yield a unique value for T_C , i.e., the latter curve gives higher value for T_C than that obtained from the former one (see inserts in Figs. 4 and 5); (iii) a higher value for the ordering temperature is obtained from a local measurement, viz., Mössbauer effect⁴² for the $\text{Fe}_{20}\text{Ni}_{60}\text{P}_{14}\text{B}_6$ alloy than the one from the present bulk magnetization measurements; (iv) M vs H curves taken at various temperatures well above T_C reveal a nonlinear relationship between magnetization and field characteristic of the superparamagnetic behavior; (v) resistivity data⁴⁵ taken on the present alloy show that above T_C

the temperature derivative of resistivity decreases very slowly over a temperature interval which is about 20 times broader than that observed in crystalline Ni or Fe; (vi) no specific-heat anomaly has been observed⁴⁵ for the alloy in question at T_C implying thereby that the spin entropy is released over a wide temperature region; and finally (vii) a superparamagnetic behavior has already been observed in parallel systems, namely, amorphous $(\text{Fe}_x\text{Ni}_{1-x})_{79}\text{P}_{13}\text{B}_8$ and $(\text{Fe}_x\text{Ni}_{1-x})_{80}\text{P}_{10}\text{B}_{10}$ alloys^{41,54} for $x \leq 0.25$.

Encouraged by such strong evidence in favor of superparamagnetism in the present alloy, magnetization-versus-field isotherms taken above T_C have been analyzed for superparamagnetic behavior. It is immediately noticed that the plots of M vs H/T do not fall on a universal curve meaning thereby that the cluster moment depends on temperature and the clusters are not independent but interact with one another. Consequently, the M vs H curves for $T \geq 228$ K have been analyzed using the relation^{55,56}

$$M(H, T) = \chi^*(T)H + \mu^*(T)c^*(T)B_s(x) \quad (11)$$

where μ^* and c^* are the average cluster moment in μ_B and number of clusters per gram, respectively, $B_s(x)$ is the Brillouin function with $x = \mu^*H/k_B T$ and $\chi^*(T)$ is a band-polarization susceptibility which is normally field independent but temperature dependent. The values of χ^* , defined as $\chi^*(T) = \lim_{H \rightarrow \infty} (dM/dH)_T$, at different temperatures evaluated from the slope of M vs H curves at the highest field value (10 kOe) are used to determine the temperature dependence of μ^* and c^* . Figure 9 shows the computed temperature dependence of μ^* , c^* , and χ^* . The salient features presented by

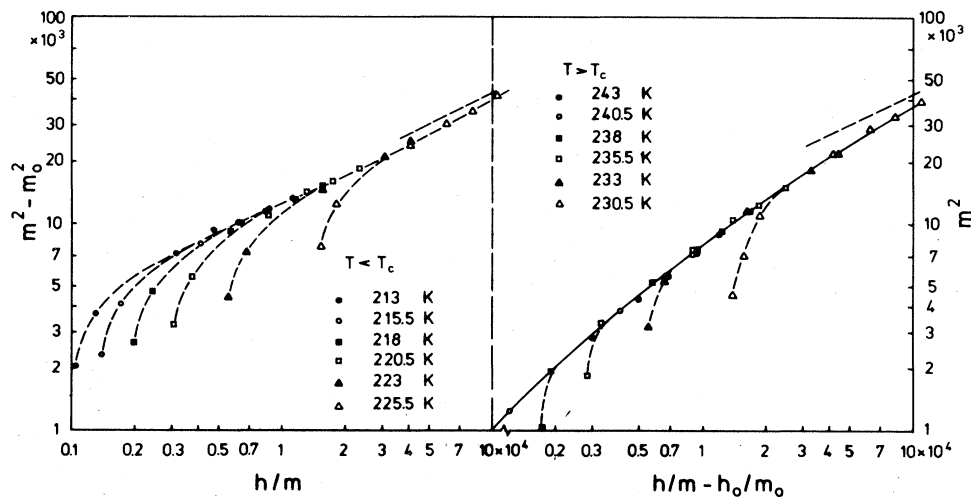


FIG. 8. log-log plots of $(m^2 - m_0^2)$ vs h/m and m^2 vs $(h/m - h_0/m_0)$ for temperatures below and above T_C , respectively. Asymptotic behavior for large m is indicated by the dashed lines. Large deviations from the asymptotic behavior for small m [see Eq. (9) of the text] are apparent for fields ≤ 700 Oe.

this figure are summarized as follows: with temperature approaching T_C from the high-temperature side, (i) the average cluster moment μ^* as a function of temperature increases at first slowly in the temperature interval 255–245 K and then steeply for temperatures below 245 K until a temperature 235 K is reached beyond which the rate of increase in its value again slows down; (ii) the average cluster concentration increases rapidly, attains a maximum value at 245 K, from 245 to 238 K falls rapidly and assumes a constant value for temperatures below 235 K; and (iii) the susceptibility χ^* decreases sharply up to 245 K, the rate of decrease slows down in the temperature interval 245–238 K and below 238 K again decreases at a fast rate which for temperatures close to T_C approaches the rate of decrease exhibited in the temperature region 255–245 K (see the dashed line in Fig. 9).

The above-mentioned findings lend themselves to a straightforward explanation which is given below. In the temperature interval 255–245 K, the superparamagnetic clusters increase in number at a much faster rate than they grow in size and the temperature dependence of χ^* is primarily governed by an increasing number of relatively small clusters whereas from 245 to 235 K two or more clusters coalesce to form a single giant cluster and consequently result in a rapid

decrease in the number of clusters and a sharp increase in the average cluster moment (formation of such giant clusters enhances the value of χ^* as is evident from the upward shift in its value relative to the dashed line and a hump in χ^* vs T curve, see Fig. 9). For temperatures below 235 K, the giant clusters neither grow in size nor increase in number but instead the moments within them get more and more ordered with lowering temperature and such a process manifests itself in a slow increase in the average cluster moment and the consequent decrease in χ^* with temperature.

Having understood the physical mechanism responsible for the observed magnetic behavior above T_C , we are now better equipped to explain the existence of a small peak in the magnetization-versus-temperature curves for fields ≤ 100 Oe and its shift to higher temperatures as the field strength is increased. It should be mentioned at this stage that similar peaks (with relatively small shift to higher temperatures with increasing field value) have been recently observed in the magnetic susceptibility of crystalline Pd-Co, (Pd₉₅Rh₅)-Co, Au-Fe, and Pd-Fe alloys^{57–60} well above their percolation limit and attributed to the onset of long-range ferromagnetic order in them. However, in the present case such an interpretation does not seem plausible for two reasons. First, of all the above-mentioned crystalline systems, the largest peak shift of about 5 K to higher temperatures in a field value of 500 Oe has been observed for Au-Fe (Ref. 59) which should be compared with the same value of peak shift (i.e., 5 K) we observe for our alloy at a field value of only 100 Oe. The obvious deduction from this comparison is that the peak shift in our case is five times as sensitive to the field as has been observed in Au-Fe system. Such a large peak shift and that, too, to higher temperatures cannot be reconciled with a long-range ferromagnetic ordering. Second, no remanence at 232 K could be detected within our experimental accuracy when the present alloy was cycled in a field of 16 kOe, an observation which clearly rules out any possibility of attributing the peak under consideration to the onset of a long-range ferromagnetic ordering in our alloy. We contend that a peak of the present type signals the freezing of ferromagnetic order within the giant superparamagnetic clusters because an appreciable shift in the peak to higher temperatures can then result from the fact that at higher temperatures higher fields are required to align the moments within the clusters and it is only when the alignment within the clusters is complete that the susceptibility exhibits the proper divergence. Furthermore, for fields ≤ 100 Oe, there could be still a sizable number of clusters sitting in hard directions and a peak in M vs T curves does not appear for fields ≥ 300 Oe since such fields are sufficient to make body rotation of the clusters possible. The dependence of the peak position T^* on

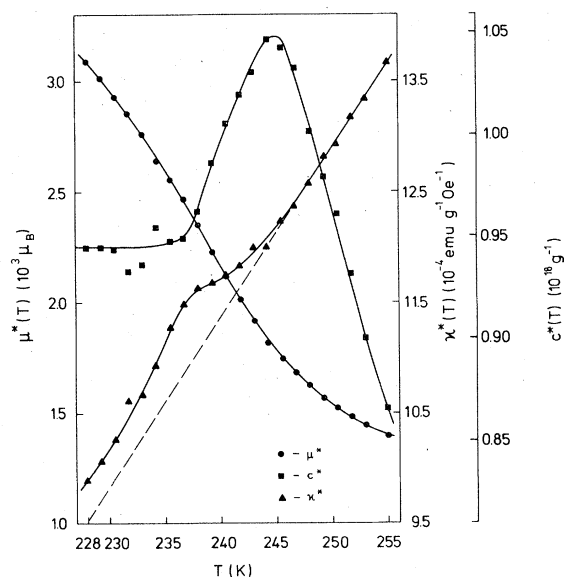


FIG. 9. Variation of the average cluster moment μ^* (closed circles), average number of clusters per gram c^* (closed squares), and field independent susceptibility χ^* (closed triangles) with temperature. The dashed line represents an extrapolation of the temperature dependence of χ^* in the temperature range 245–255 K to lower temperatures.

field is shown in the left-hand-side insert of Fig. 1. Since the peak in M vs T curves shifts to higher temperatures by about 2.5 K when the field strength is doubled, a parabolic extrapolation (dashed curve) through the data points is used to find the value of T^* at $H=0$. Such a procedure gives $T^*(H=0)$ with the error limits as 233 ± 1 K.

The overall physical picture that emerges from the present investigation can be summarized as follows: with temperature decreasing from $T \gg 255$ K, many of the randomly positioned and freely rotating spins build themselves into clusters which can then grow in size and rotate as a whole. Further decrease in temperature results in not only increasing the number of such clusters and decreasing their relaxation rate but also in making a ferromagnetic interaction, which progressively builds up in strength, operate between them on a microscopic scale until a temperature ~ 245 K is reached when the number of such newly formed clusters no longer increases but instead the ferromagnetic interaction between the statistical near-neighbor clusters on a microscopically localized scale becomes so strong as to make two or more of such clusters merge into one another to form a single giant cluster. The formation of giant clusters causes overall thermal relaxation rate of the clusters to decrease very rapidly since the individual clusters forming a giant cluster possess a much shorter relaxation time than that possessed by the giant cluster after it has been formed. A process of this type continues till $T \sim 237$ K below which the moments within the giant clusters get more and more ordered since by the time a temperature ~ 237 K is reached, the thermal relaxation rate of the giant clusters has slowed down considerably. At a temperature ~ 234 K, the relaxation time of the giant clusters becomes long enough compared with the lifetime of the Mössbauer transition ($\sim 10^{-8}$ sec) (the latter measurement can now detect the short-range order within them) and the Mössbauer spectrum of Fe appears.⁴² Around 232 K the ferromagnetic order within the clusters freezes whereas below this temperature a long-range ferromagnetic interaction between the giant clusters is suddenly switched on so as to form an infinite cluster with an infinite chain of near-neighbor Fe atoms (note that for nickel-rich amorphous alloys, Ni possesses negligible or zero moment⁴²). The onset of a long-range ferromagnetic ordering in the present alloy is marked by a steep rise in magnetization below 232 K to very large values and a knee in M vs T curves at $T \sim 228$ K (see Fig. 1). Another observation in support of the above statement is that a hysteresis loop (with a saturation magnetization value of 49.5 emu/g) characteristic of ferromagnetics in the amorphous state was observed at 77 K when the alloy was cycled in a field of 16 kOe. In view of the foregoing text, it is not surprising to note that the first temperature derivative of alloy resistivity gives the

ordering temperature as 230 K since at that temperature the size of the clusters greatly exceeds the mean-free path of the conduction electrons (a situation when the spin-disorder scattering is appreciably reduced) and a change in the slope of resistivity-versus-temperature curve results.

Finally, it should be remarked in the passing that the values for the critical exponents determined in the present work could be influenced to a small extent by the presence of giant superparamagnetic clusters above T_C . The above statement is true, in particular, for the critical exponent β since presence of such clusters gives rise below T_C to appreciable non-linearity in the Arrott plots which, in turn, could result in some error in the determination of β in spite of the best efforts to minimize the same. The observation that the presently determined exponent values are in close agreement (except for β) with those obtained previously for the so-called "Fe-Ni phase" in Metglas 2826A (Ref. 33) lends further support to this viewpoint. Therefore, more experimental data on a number of other amorphous magnetic alloys are needed to establish the trend that for magnetic alloys in the amorphous state the value of β is close to 0.4 rather than to the Heisenberg value of 0.37.

III. SUMMARY

Exhaustive magnetization data taken in the critical region of the amorphous $\text{Fe}_{20}\text{Ni}_{60}\text{P}_{14}\text{B}_6$ alloy when analyzed with caution enables us to arrive at reliable values for the critical exponents. The exponent values are found to follow closely the predictions of a three-dimensional Heisenberg model. This observation points to the fact that the short-range forces dominate in the critical region. Long-range forces, e.g., dipolar forces, have been shown to have negligible influence on the critical fluctuations of magnetization. A detailed analysis, which allows for changes in the average cluster moment and cluster concentration with temperature, of the experimental data taken above T_C reveals the existence of giant superparamagnetic clusters. The physical basis for observing different values for the ferromagnetic ordering temperature as determined by Mössbauer effect on one hand, and resistivity and the present magnetization measurements on the other, has been provided. In conclusion, the present alloy is an inhomogeneous long-range ferromagnet and represents a composition in the alloy series $\text{Fe}_x\text{Ni}_{80-x}\text{P}_{14}\text{B}_6$ just above the percolation limit.

ACKNOWLEDGMENTS

The author is grateful to Professor M. Rosenberg for many fruitful discussions and for kindly providing the present sample. Thanks are also due to Professor S. Methfessel for kindly permitting the author to carry out the present investigation in his institute.

- ¹M. E. Fisher, *J. Math. Phys.* **4**, 278 (1963); **5**, 944 (1964).
- ²L. P. Kadanoff, W. Götze, D. Hamblen, R. Hecht, E. A. S. Lewis, V. V. Palciauskas, M. Rayl, J. Swift, D. Aspnes, and J. Kane, *Rev. Mod. Phys.* **39**, 395 (1967); P. Heller, *Rep. Prog. Phys.* **30**, 731 (1967).
- ³M. E. Fisher, *Phys. Rev.* **176**, 257 (1968).
- ⁴H. E. Stanley, *Introduction to Phase Transitions and Critical Phenomena* (Clarendon, Oxford, 1971), and references cited therein.
- ⁵K. Binder and H. Müller-Krumbhaar, *Phys. Rev. B* **7**, 3297 (1973).
- ⁶M. E. Fisher, *Rev. Mod. Phys.* **46**, 597 (1974).
- ⁷A. B. Harris, *J. Phys. C* **7**, 1671 (1974).
- ⁸A. B. Harris and T. C. Lubensky, *Phys. Rev. Lett.* **33**, 1540 (1974).
- ⁹G. S. Rushbrooke, G. A. Baker, Jr., and P. J. Wood, in *Phase Transitions and Critical Phenomena*, edited by C. Domb and M. S. Green (Academic, New York, 1974), Vol. 3, p. 245, and references cited therein.
- ¹⁰C. Domb, in Ref. 9, p. 357, and the references quoted therein.
- ¹¹T. C. Lubensky and A. B. Harris, in *Magnetism and Magnetic Materials—1974*, edited by C. D. Graham, G. H. Lander, and J. J. Rhyne, AIP Conf. Proc. No. 24 (AIP, New York, 1975), p. 311.
- ¹²U. Krey, *Phys. Lett. A* **51**, 189 (1975).
- ¹³G. Grinstein and A. Luther, *Phys. Rev. B* **13**, 1329 (1976).
- ¹⁴H. Müller-Krumbhaar, *J. Phys. C* **9**, 345 (1976), and references cited therein.
- ¹⁵L. P. Kadanoff, in *Phase Transitions and Critical Phenomena*, edited by C. Domb and M. S. Green (Academic, New York, 1976), Vol. 5A, p. 1, and the references quoted therein.
- ¹⁶K. Binder, in *Phase Transitions and Critical Phenomena*, edited by C. Domb and M. S. Green (Academic, New York, 1976), Vol. 5B, p. 1, and the references cited therein.
- ¹⁷J. S. Kouvel and M. E. Fisher, *Phys. Rev.* **136**, A1626 (1964).
- ¹⁸R. V. Colvin and S. Arajs, *J. Phys. Chem. Solids* **26**, 435 (1965).
- ¹⁹J. S. Kouvel and D. S. Rodbell, *Phys. Rev. Lett.* **18**, 215 (1967).
- ²⁰A. Arrott and J. E. Noakes, *Phys. Rev. Lett.* **19**, 786 (1967).
- ²¹J. S. Kouvel and J. B. Comly, *Phys. Rev. Lett.* **20**, 1237 (1968).
- ²²M. F. Collins, V. J. Minkiewicz, R. Nathans, L. Passell, and G. Shirane, *Phys. Rev.* **179**, 417 (1969).
- ²³S. Arajs, B. L. Tehan, E. E. Anderson, and A. A. Stelmach, *Int. J. Magn.* **1**, 41 (1970).
- ²⁴M. N. Deschizeaux and G. Develley, *J. Phys. (Paris)* **32**, 319 (1971).
- ²⁵C. J. Glinka, V. J. Minkiewicz, and L. Passell, in *Magnetism and Magnetic Materials—1974*, edited by C. D. Graham, G. H. Lander, and J. J. Rhyne, AIP Conf. Proc. No. 24 (AIP, New York, 1975), p. 283.
- ²⁶T. Mizoguchi and K. Yamauchi, *J. Phys. (Paris)* **35**, C4-287 (1974).
- ²⁷K. Yamada, Y. Ishikawa, Y. Endoh, and T. Masumoto, *Solid State Commun.* **16**, 1335 (1975).
- ²⁸T. Mizoguchi, in *Magnetism and Magnetic Materials—1976*, edited by J. J. Becker and G. H. Lander, AIP Conf. Proc. No. 34 (AIP, New York, 1976), p. 286.
- ²⁹E. Figueroa, L. Lundgren, O. Beckman, and S. M. Bhagat, *Solid State Commun.* **20**, 961 (1976), and the references quoted therein.
- ³⁰S. J. Poon and J. Durand, *Phys. Rev. B* **16**, 316 (1977).
- ³¹L. J. Schowalter, M. B. Salamon, C. C. Tsuei, and R. A. Craven, *Solid State Commun.* **24**, 525 (1977).
- ³²R. Malmhäll, G. Bäckström, K. V. Rao, S. M. Bhagat, M. Meichle, and M. B. Salamon, *J. Appl. Phys.* **49**, 1727 (1978), and the references cited therein.
- ³³S. N. Kaul, *Phys. Rev. B* **22**, 278 (1980).
- ³⁴S. Milosevic and H. E. Stanley, *Phys. Rev. B* **6**, 986 (1972).
- ³⁵C. Domb and D. L. Hunter, *Proc. Phys. Soc. London* **86**, 1147 (1965).
- ³⁶B. Widom, *J. Chem. Phys.* **43**, 3898 (1965).
- ³⁷L. P. Kadanoff, *Physics* **2**, 263 (1966).
- ³⁸S. N. Kaul, *Solid State Commun.* (in press).
- ³⁹T. E. Sharon and C. C. Tsuei, *Solid State Commun.* **9**, 1923 (1971); *Phys. Rev. B* **5**, 1047 (1972).
- ⁴⁰R. Hasegawa, *J. Appl. Phys.* **41**, 4096 (1970); *J. Phys. Chem. Solids* **32**, 2487 (1971).
- ⁴¹J. Durand, in *Amorphous Magnetism II*, edited by R. A. Levy and R. Hasegawa (Plenum, New York, 1977), p. 305, and the references quoted therein; see also S. J. Poon and J. Durand, *ibid.*, p. 245.
- ⁴²C. L. Chien, D. P. Musser, F. E. Luborsky, J. J. Becker, and J. L. Walter, *Solid State Commun.* **24**, 231 (1977), and the references quoted therein.
- ⁴³D. G. Onn, T. H. Antoniuk, T. A. Donnelly, W. D. Johnson, T. Egami, J. T. Prater, and J. Durand, *J. Appl. Phys.* **49**, 1730 (1978).
- ⁴⁴H. Gudmundsson, K. V. Rao, A. C. Anderson, B. Brandt, and T. Egami, *J. Appl. Phys. Abstr.* **50**, 7373 (1979).
- ⁴⁵Z. Marohnic, K. Saub, E. Babic, and J. Ivkov, *Solid State Commun.* **30**, 651 (1979), and the references cited therein; E. Babic, B. Fogarassy, T. Kemeny, Z. Marohnic, and K. Saub (private communication).
- ⁴⁶J. J. Becker, F. E. Luborsky, and J. L. Walter, *IEEE Trans. Magn.* **13**, 988 (1977), and the references quoted therein.
- ⁴⁷A. Arrott, *Phys. Rev.* **108**, 1394 (1957).
- ⁴⁸J. S. Kouvel, General Electric Lab. Report No. 57-RL-1799, 1957 (unpublished).
- ⁴⁹W. Rucker and R. Kohlhaas, *Z. Angew. Phys.* **23**, 146 (1967).
- ⁵⁰S. Arajs, C. A. Moyer, and K. W. Brown, *Phys. Scr.* **17**, 543 (1978), and the references quoted therein.
- ⁵¹P. G. de Gennes, *J. Phys. Rad.* **23**, 630 (1962); T. Kaneyoshi, *J. Phys. F* **5**, 1014 (1975).
- ⁵²J. S. Kouvel, in *Magnetism in Alloys*, edited by P. A. Beck and J. T. Waber (American Institute of Mining, Metallurgical, and Petroleum Engineers, U.S.A., 1972), p. 165, and the references quoted therein.
- ⁵³W. C. Mueller and J. S. Kouvel, *Phys. Rev. B* **11**, 4552 (1975); D. Sain and J. S. Kouvel, *ibid.* **17**, 2257 (1978), and the references quoted therein.
- ⁵⁴J. Schneider, K. Zaveta, A. Handstein, R. Hesske, and W. Haubenreisser, *Physica* **91B**, 185 (1977); J. Schneider, K. Zaveta, A. Handstein, F. Zounova, and V. Nekvasil, *Phys. Status Solidi A* **56**, K141 (1979), and the references cited therein.
- ⁵⁵P. A. Beck, in *Magnetism in Alloys*, edited by P. A. Beck and J. T. Waber (American Institute of Mining, Metal-

- lurgical, and Petroleum Engineers, U.S.A., 1972), p. 211, and the references quoted therein.
- ⁵⁶P. A. Beck, *J. Less-Common Met.* 28, 193 (1972), and the references cited therein; P. A. Beck and D. J. Chakrabarti, in *Amorphous Magnetism*, edited by H. O. Hooper, and A. M. de Graaf (Plenum, New York, 1973), p. 273.
- ⁵⁷I. Maartense and G. Williams, *J. Phys. F* 6, L121 (1976).
- ⁵⁸I. Maartense and G. Williams, *J. Phys. F* 6, 2363 (1976).
- ⁵⁹I. Maartense and G. Williams, *Phys. Rev. B* 17, 377 (1978), and the references quoted therein.
- ⁶⁰B. H. Verbeek, G. J. Nieuwenhuys, H. Stocker, and J. A. Mydosh, *J. Phys. (Paris)* 39, C6-916 (1978), and the references cited therein.